TECHNICAL REPORT STANDARD PAGE

1. Title and Subtitle

Elimination of End Zone Cracks in Precast Prestressed Concrete Girders Using Shape Memory Alloys

2. Author(s)

C. Shawn Sun

3. Performing Organization Name and Address

Civil Engineering Program
Louisiana Tech University
Ruston, LA 71270

4. Sponsoring Agency Name and Address

Louisiana Department of Transportation and Development
P.O. Box 94245
Baton Rouge, LA 70804-9245

5. Report No.

FHWA/LA.17/Enter 3-digit Report No.

6. Report Date

December 31, 2020

7. Performing Organization Code

LTRC Project Number: 20-4TIRE
SIO Number: DOTLT1000301

8. Type of Report and Period Covered

Final Report
07/2019 – 12/2020

9. No. of Pages

45

10. Supplementary Notes

11. Distribution Statement

12. Key Words

13. Abstract

Precast prestressed concrete girders have been widely used to construct bridges in the United States. Recent advancements in high-performance concrete and newly developed girder sections, such as LG girders in Louisiana, allow girders' spans to be extended significantly. Generally, bridges with longer spans require deeper girders and use more prestressing strands; the latter exacerbates the end zone cracking in pretensioned concrete girders when the prestressing strands are released. These cracks may affect the girders' durability adversely and even cause girder rejection by bridge owners. The current practice is to control the cracks to an acceptable extent by providing sufficient end zone reinforcement. However, the end zone cracks cannot be eliminated, primarily because the girders are prestressed along their length only, i.e., there is no prestressing along the girder's height. As a result, the bursting force at the time of prestress release causes the girder ends to crack. To resolve the problem of end zone cracking thoroughly, this report proposes an innovative method to provide vertical prestressing at the girder ends using shape memory alloys (SMAs). SMAs are characterized by a solid-solid, reversible phase

transformation between two primary microstructural phases, martensite and austenite. SMAs exist in the martensite phase at relatively low temperatures and undergo a transformation to the austenite phase when heated. When prestrained SMAs are heated at a concrete beam end, the recovery stress can result in vertical prestress that contributes to increase the splitting resistance and avoid the web cracking. NiTi SMA wires, strands, and cables were used to demonstrate the feasibility in producing prestressing through small-scale beam tests and a full-scale beam test. Test results showed that the vertical prestress, when properly designed, can be sufficient to overcome the bursting force and eliminate concrete cracks.

Project Review Committee

Each research project will have an advisory committee appointed by the LTRC Director. The Project Review Committee is responsible for assisting the LTRC Administrator or Manager in the development of acceptable research problem statements, requests for proposals, review of research proposals, oversight of approved research projects, and implementation of findings.

LTRC appreciates the dedication of the following Project Review Committee Members in guiding this research study to fruition.

LTRC Administrator/Manager
Vijaya (VJ) Gopu, Ph.D., P.E.
Associate Director, External Programs

Members
Enter member's names, one per line

Directorate Implementation Sponsor
Christopher P. Knotts, P.E.
DOTD Chief Engineer

Elimination of End Zone Cracks in Precast Prestressed Concrete Girders Using Shape Memory Alloys

By

C. Shawn Sun

Civil Engineering Program

Louisiana Tech University

Ruston, LA 71272

December 31, 2020

Abstract

Precast prestressed concrete girders have been widely used to construct bridges in the United States. Recent advancements in high-performance concrete and newly developed girder sections, such as LG girders in Louisiana, allow girders' spans to be extended significantly. Generally, bridges with longer spans require deeper girders and use more prestressing strands; the latter exacerbates the end zone cracking in pretensioned concrete girders when the prestressing strands are released. These cracks may affect the girders' durability adversely and even cause girder rejection by bridge owners. The current practice is to control the cracks to an acceptable extent by providing sufficient end zone reinforcement. However, the end zone cracks cannot be eliminated, primarily because the girders are prestressed along their length only, i.e., there is no prestressing along the girder's height. As a result, the bursting force at the time of prestress release causes the girder ends to crack. To resolve the problem of end zone cracking thoroughly, this report proposes an innovative method to provide vertical prestressing at the girder ends using shape memory alloys (SMAs). SMAs are characterized by a solid-solid, reversible phase transformation between two primary microstructural phases, martensite and austenite. SMAs exist in the martensite phase at relatively low temperatures and undergo a transformation to the austenite phase when heated. When prestrained SMAs are heated at a concrete beam end, the recovery stress can result in vertical prestress that contributes to increase the splitting resistance and avoid the web cracking. NiTi SMA wires, strands, and cables were used to demonstrate the feasibility in producing prestressing through small-scale beam tests and a full-scale beam test. Test results showed that the vertical prestress, when properly designed, can be sufficient to overcome the bursting force and eliminate concrete cracks.

Acknowledgments

Implementation Statement

This project proposes an innovative solution to eliminate the end zone cracks in precast prestressed concrete girders. Prestrained SMAs can be placed at a girder end to result in vertical prestress when they are electrically heated. The resulting prestressing force can increase the splitting resistance and avoid web cracking. NiTiNb strands or cables are suitable to be used at the ends of precast prestressed concrete girders.

Table of Contents

List of Tables

List of Figures

Introduction

Precast prestressed concrete girders have been used widely to construct bridges in the United States. Recent advancements in high-performance concrete and newly developed girder sections, such as LG girders in Louisiana, allow girders' spans to be extended significantly. Generally, bridges with longer spans require deeper girders and use more prestressing strands; the latter exacerbates the end zone cracking in pretensioned concrete girders when the prestressing strands are released. Various types of end zone cracks have been observed, including horizontal and inclined cracks in the web, and bottom flange cracks (Figure 1). These cracks may affect the girders' durability adversely, especially when chloride ions can penetrate into the reinforcement and cause corrosion concerns.

Figure 1. End zone cracks in a prestressed concrete beam [1]

Numerous studies, including NCHRP Report 654 by Tadros et al. [2], have been conducted on the evaluation and repair of end zone cracking. The current practice is to control the cracks to an acceptable extent by providing sufficient end zone reinforcement. In accordance with the current AASHTO LRFD Bridge Design Specifications [3], vertical reinforcement shall be provided to resist four percent of the total prestressing force at prestress release and be located as close to the girder end as possible. When the girders include a large number of prestressing strands, congested reinforcing details are mandatory to control the cracks. More importantly, the end zone cracks cannot be eliminated, primarily because the girders are prestressed along their length only, i.e.,

there is no prestressing along the girder's height. As a result, the bursting force at the time of prestress release causes the girder ends to crack. To resolve the problem of end zone cracking thoroughly, this report presents an innovative method to provide vertical prestressing at the girder ends using shape memory alloys (SMAs).

Literature Review

SMAs are characterized by a solid-solid, reversible phase transformation between two primary microstructural phases, martensite and austenite [4]. SMAs' uniqueness rests in their ability to undergo large deformations and return to their undeformed shape by eliminating stress (superelasticity) or by heating (shape memory effect) [5]. SMAs exist in the martensite phase at relatively low temperatures and undergo a transformation to the austenite phase when heated. The following four distinct transformation temperatures characterize SMAs (Figure 2): martensite start (M_s), martensite finish (M_f), austenite start (A_s), and austenite finish (A_f). SMA exists in a fully martensite state when its temperature is less than M_f and in a fully austenite state when its temperature is greater than A_f.

Figure 2. Phase transformation and change in SMAs' crystalline structure as a function of temperature [5]
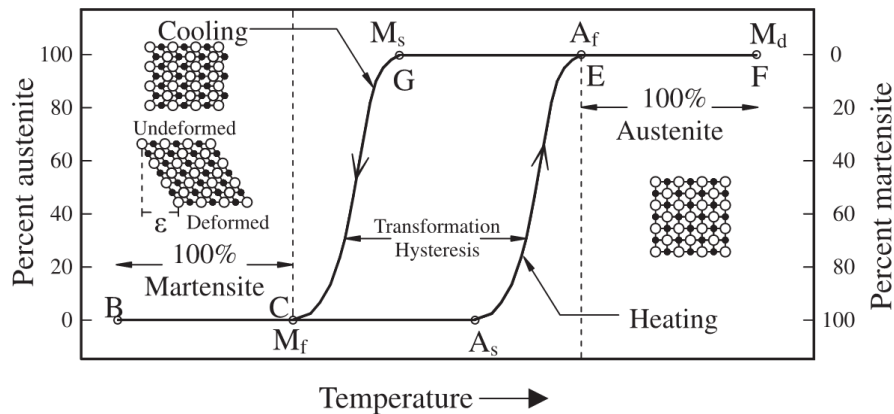
SMAs' mechanical properties differ substantially depending on the constitutive metals' relative proportions. Commonly used SMAs in civil engineering structures include NiTi, NiTiNb, and iron-based SMAs. Maji and Negret were the first to use the shape memory effect in NiTi SMAs to induce prestressing in concrete beams [6]. SMA strands were pretensioned under the strain-hardening regime and then embedded in model mortar beams. After the beams were cured, the SMA strands were activated with heat.

El-Tawil and Ortega-Rosales tested small mortar beams that were prestressed using SMA tendons [7]. Prestrained SMA tendons were placed in mortar beams and heated to result in the prestressing effect. Four-point loading beam tests showed that a significant level of prestressing force was attained in the beams (Figure 3). They studied both 2.5 mm-diameter NiTi and 6.3 mm-diameter NiTiNb wires. The NiTi wires exhibited appreciable constrained recovery stress, but all recovery stress was lost once the heat was removed. The NiTiNb wires appeared to be more suitable for permanent prestressing applications.

Figure 3. Four-point bending test [7]

Sherif et al. studied the use of SMAs to self-post-tension concrete beams by taking advantage of the grout's heat of hydration [8]. They examined the temperature increase due to heat of hydration of four commercial grouts and explored the feasibility of activating NiTiNb alloys. A recovery stress of over 500 MPa was accomplished after cooling to ambient temperature.

Moser et al. evaluated the feasibility of prestressing concrete beams using SMA short fibers [9]. They shaped the SMA wires by inelastic elongation into loop- and star-shaped fibers. Mortar prisms were made by including multiple layers of SMA fibers (Figure 4). After the mortar hardened, the specimens were heated to activate the SMAs and the recovery stress introduced prestress to the specimens. As a result, the specimens were subject to compressive stresses up to 7 MPa.

Figure 4. Multiple layers of SMA fibers in a mortar prism [9]
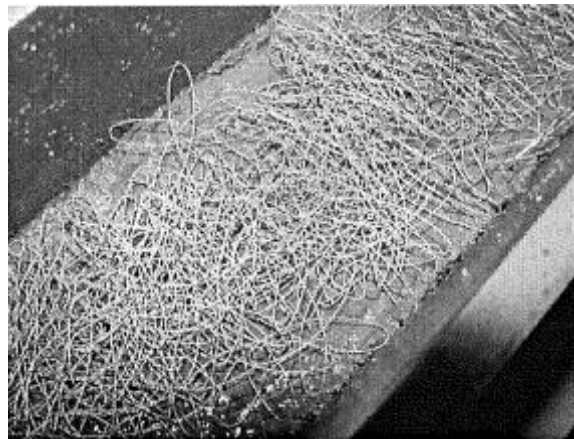
Soroushian et al. conducted repair and strengthening of concrete members using iron-based SMAs [10]. They found that the alloys could introduce post-tensioning forces to structural systems. SMA rods were adopted to transfer corrective forces to concrete beams for repair and strengthening. This concept was implemented to strengthen the bridge beams that had insufficient shear strength (Figure 5).

Figure 5. Beam repair using SMA rods [10]

Andrawes developed an Adaptive Prestressing System (APS) for concrete crossties using SMAs [11]. NiTiNb SMA wires were used to prestress concrete crossties at target regions. A variety of SMA prestressing system configurations were tested, including straight, L-shaped, and U-shaped wires. The test results confirmed that the SMA wires were capable of inducing prestressing forces at the specified locations of the crossties. Figure 6 shows the SMA wire assembly and test setup of a concrete crosstie specimen.

Figure 6. SMA wire assembly and test setup of a concrete crosstie [11]
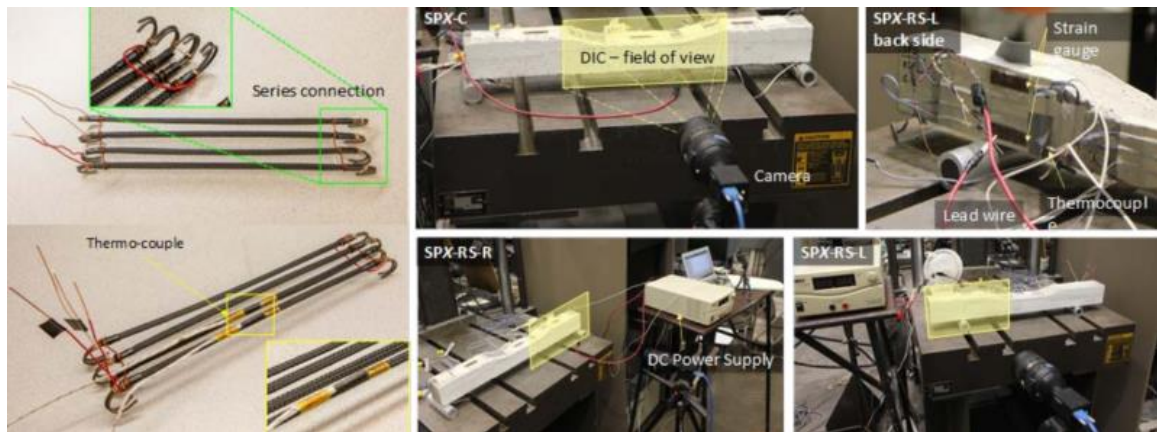
Sinha et al. proposed a post-tensioning technique using unbonded near-surface mounted NiTiNb SMA wires [12]. The wires with 2.5% prestrain resulted in a recovery stress of about 500 MPa after being Ohmic heated in a restrained condition. They installed the SMA wires on pre-cracked concrete girders to assess the prestressing effect when the wires were heated (Figure 7). As a result, the crack widths were reduced by up to 74%.

Figure 7. Pre-cracked concrete girder detail [12]
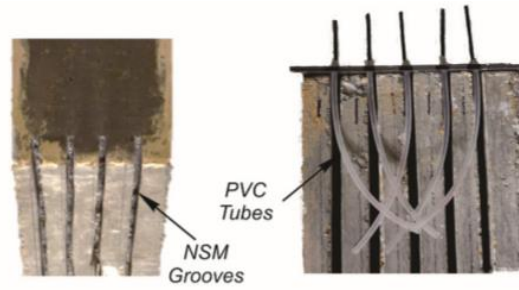
A number of researchers have explored the feasibility of introducing prestressing to concrete beams using SMAs. The application of SMAs has been related to either new construction or repair/strengthening of concrete members. However, the use of SMAs at the end zone of prestressed concrete girders has not been evaluated yet. This study presents the first attempt to study its feasibility of increasing splitting resistance in prestressed concrete girders.

Objective

The research objective is to examine the feasibility of using SMAs to eliminate the end zone cracks in precast prestressed concrete girders.

Scope

This project included four tasks: literature review, small-scale beam tests, full-scale beam test, and finite element analysis. A literature review was performed to present the current studies of SMAs on how to induce prestressing in concrete members. Small-scale beams were made to study the effectiveness of SMA wires, strands, and cables in generating a meaningful level of prestressing. A full-scale prestressed concrete I-beam was produced to evaluate the feasibility of using SMAs at the beam end. In addition to the steel strands at both beam flanges, SMA wires and cables were included to result in vertical prestress. Strain gauges were installed in the beam web to capture its response at the time of heating the SMAs and at prestress release. Finite element analysis was conducted to simulate the behavior of the beam end.

Methodology

Experimental Study

A number of suppliers were contacted to order NiTi and NiTiNb SMAs. Unfortunately, a majority of the suppliers can only provide small-diameter wires and no suitable NiTiNb SMAs were available. As a result, NiTi SMA wires, strands, and cables from one supplier were used in this project. Table 1 lists the SMA wire, strand, and cable, their descriptions, cross sectional areas, and A_f.

The experimental study included tension tests of the wires, strands, and cables to determine their primary mechanical properties. Prestrained wires, strands, and cables were used in small-scale beams to explore the feasibility of introducing prestressing. Based on the findings of the small-scale beam tests, a full-scale beam was made to study the effectiveness of SMA wires and cables in providing splitting resistance at the beam end.

Table 1. List of SMA wire, strand, and cable

Item	Description	Area (in.²)	A_f (ºC)
Wire	0.0787 in. diameter	0.0049	94
Strand	7-wire strand; 0.11 in. diameter	0.0074	65
Cable	7-strand cable; 0.33 in. diameter	0.0520	65

Tension Tests of SMA Wires, Strands, and Cables

An MTS machine was used to determine the stress-strain responses of SMA wires and strands up to failure. Figure 8 (a) and (b) show the testing of a wire before and after the failure, respectively. The test setup for the strand is shown in Figure 9. The clear length of the wire and strand between the grips was approximately 10 in. When the wire or strand was loaded, a displacement-control option was used with a loading rate of 0.2 in. per minute. An initial force of 20 lbs was applied to eliminate the sag in the samples. The stress-strain diagrams of the wire and strand are plotted in Figure 10 and Figure 11, respectively. The wires reached an ultimate strength of approximately 155 ksi with a corresponding strain of about 13%. The ultimate strength of the strand was about 174 ksi with an ultimate strain of approximately 11%.

Because the grips in the MTS machine cannot accommodate the SMA cable, its tensile strength was estimated using a hydraulic mono-strand jack. Ultra-high strength concrete (UHPC) blocks were placed side by side and the cable was pulled through the slots in the blocks. One end of the cable was anchored by a chuck, while the other end was tensioned by the jack (Figure 12). Two cables were tested to failure when the loads reached approximately 8.6 kips.

Figure 8. Testing of a SMA wire

(a). Preparation of the tension test (b) Tensile failure of the wire

Figure 9. Testing of a SMA strand
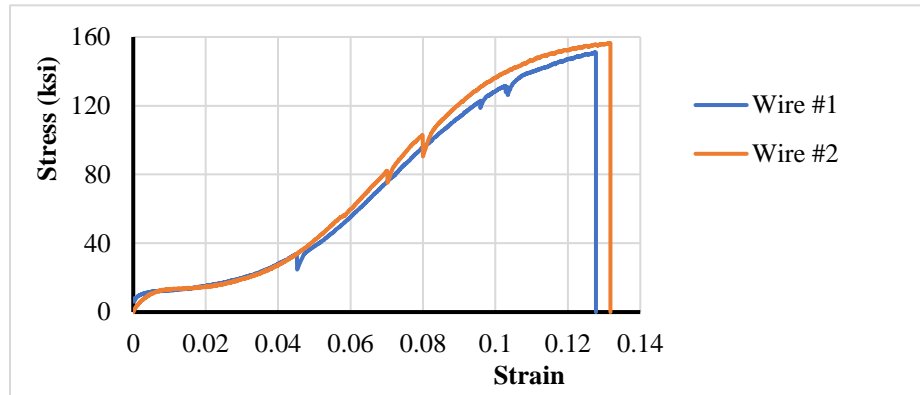
Figure 10. Stress-strain diagram of SMA wire

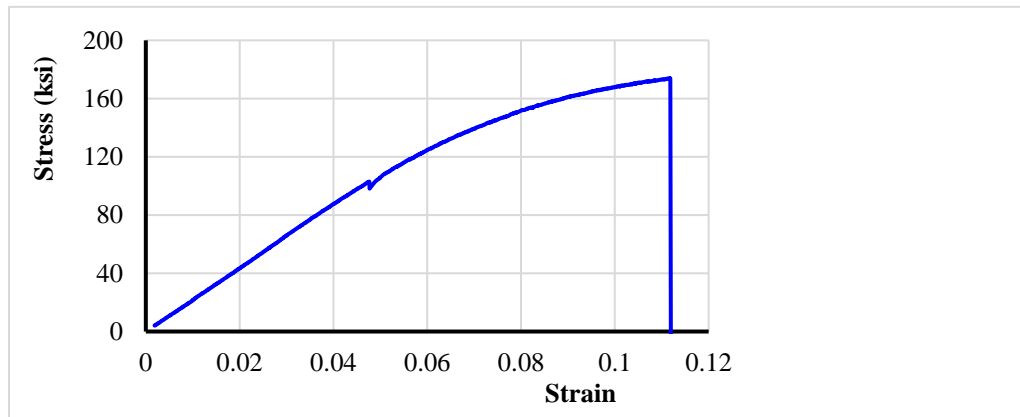**Figure 11. Stress-strain diagram of SMA strand**

Figure 12. Testing of a SMA cable

Prestrained SMA Wires, Strands, and Cables

At room temperature, the wires and strands were loaded and unloaded using the MTS machine to introduce residual strains. The maximum stresses introduced in the wires and strands were slightly lower than their ultimate tensile strengths to maximize the residual strains. During the unloading process, a force-control option was used with a rate of 5 lbs per second. As a result, approximately 8% and 2% residual strains were introduced in the wires and strands, respectively. Figure 13 and Figure 14 plot the stress-strain diagrams of the wires and strands subject to loading and unloading. Five wires and five strands were tested and comparable plots were achieved among each type of samples. Similarly, the SMA cables were tensioned to 7.8 kips using the mono-strand jack and then released to result in residual strains. As a result, the residual strains in the cables reached approximately 1.7%.

Figure 13. Stress-strain diagrams of SMA wires due to loading and unloading
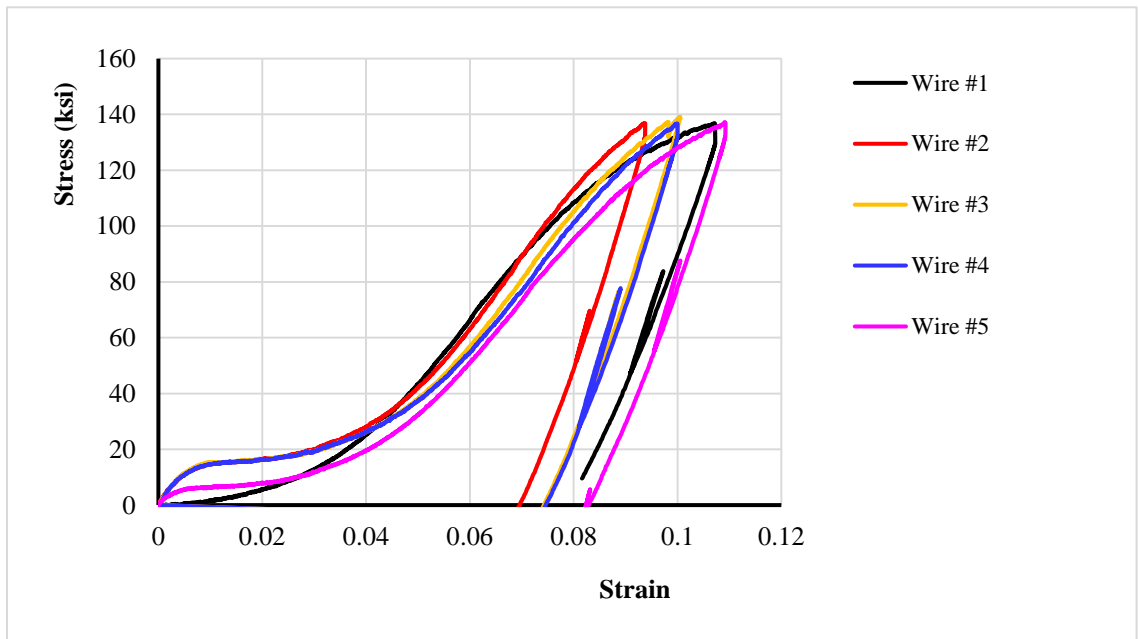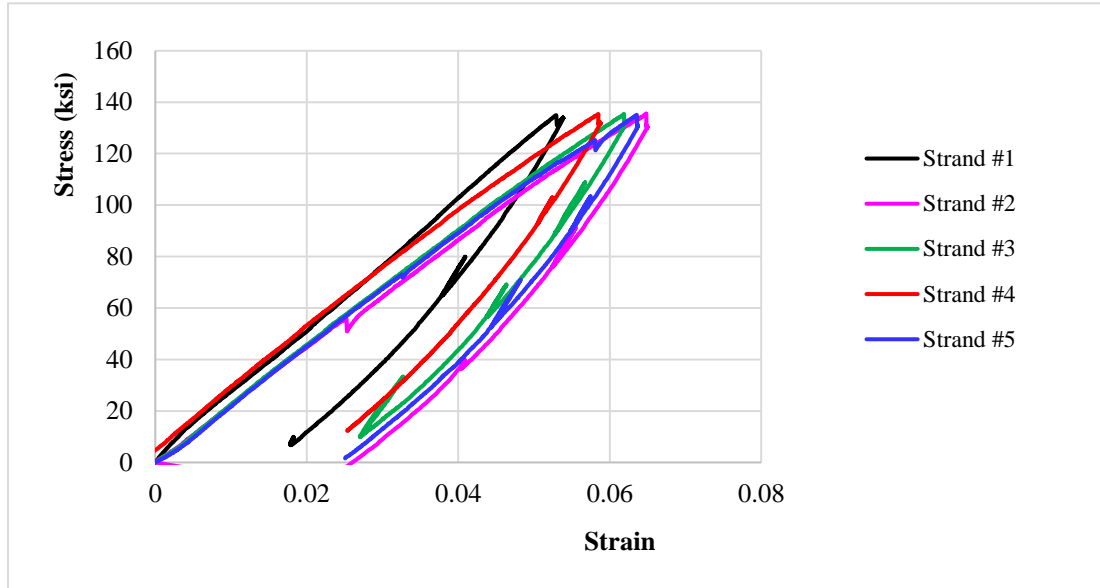
Figure 14. Stress-strain diagrams of SMA strands due to loading and unloading

Small-scale Beam Tests

To investigate the feasibility of introducing prestressing in concrete beams, prestrained NiTi wires, strands, and cables were placed in small-scale beams made of either Type-M mortar or concrete. The SMA reinforcement was either bonded or unbonded with the mortar or concrete. Table 2 summarizes the beams, SMA types, use of mortar or concrete, beam cross section dimensions, beam lengths, and bonded or unbonded SMA types. Figure 15 shows the formwork for 2 in.-cube specimens made of mortar. The following sections describe various types of specimens and their test results.

Table 2. List of small-scale beams

Beam No.	SMA type	Mortar or concrete	Beam section	Beam length	Bonded or unbonded
1	Two wires	Mortar	1 in. x 1 in.	12 in.	Bonded
2	One strand	Mortar	1 in. x 1 in.	12 in.	Bonded
3	One cable	Concrete	2 in. x 2 in.	12 in.	Unbonded
4	One cable	Concrete	2 in. x 2 in.	12 in.	Bonded

Figure 15. Formwork for 2-in. cube specimens made of mortar
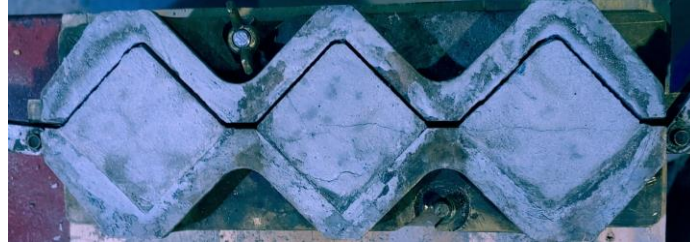
The test setup of Beam No. 1 is shown in Figure 16, in which two SMA wires were bundled and bonded with the mortar. One strain gauge was provided at each side face of the beam to measure the axial strain of the beam. Figure 17 plots the average readings from the two gauges versus time. A significant drop of the strain readings was captured at the time of approximately 800 seconds, which was caused by the recovery stress of the wire after being electrically heated. The beam had a maximum compressive strain of approximately 250 microstrain. The strains gradually increased afterward, partially because the concrete was heated up and expanded. When the concrete temperatures dropped slowly, the beam re-gained some compressive strains. When the concrete temperature stabilized at the end, the compressive strain was approximately 160 microstrain.

Figure 16. Test setup of Beam No. 1

Figure 17. Test results of Beam No. 1

Figure 18 shows the test setup of Beam No. 2, in which one SMA strand was bonded with the mortar. One strain gauge was installed at each side face of the beam. The average readings from the two gauges versus time were plotted in Figure 19 after electrically heating the strand. The beam exhibited a maximum compressive strain of approximately 140 microstrain when the strand was activated. When the concrete temperature returned to room temperature, the compressive strain was approximately 40 microstrain, i.e., a significant portion of the recovery stress was lost.

Figure 18. Test setup of Beam No. 2

Figure 19. Test results of Beam No. 2
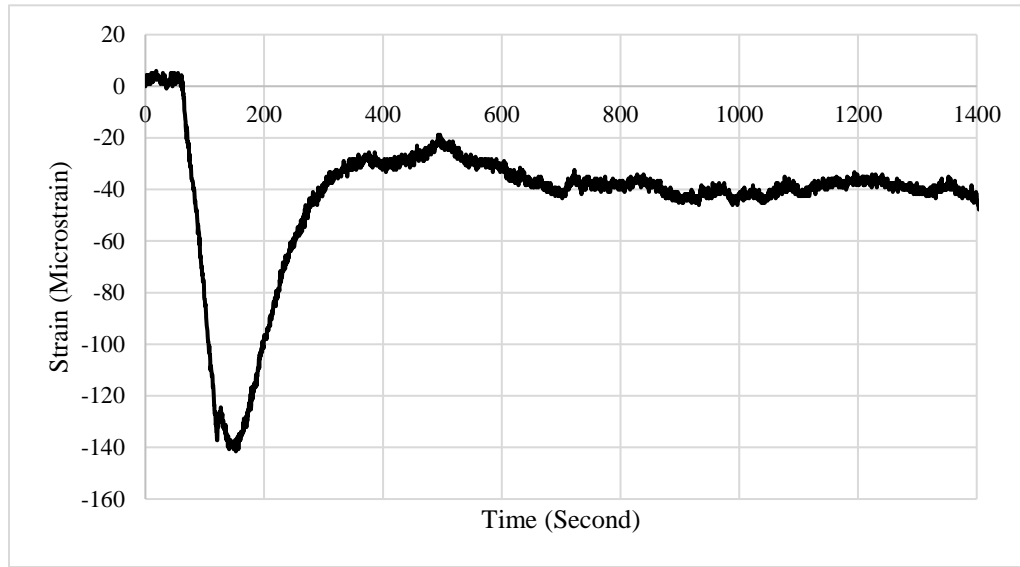
Figure 20 shows the test setup of Beam No. 3, in which one SMA cable was housed in a PVC pipe and unbonded with the concrete. The cable was anchored by a chuck at each beam end. One anchor was fully seated when the cable was prestrained. When the other anchor was installed to the beam, the cable was re-tensioned to approximately 770 lbs to remove the anchor set loss. One strain gauge was placed at each side face of the beam. Figure 21 plots the average readings from the two gauges versus time. When the cable was electrically heated, the beam was subject to a maximum compressive strain of 50 microstrain, which corresponded to about 174 psi compressive stress in the concrete beam. This indicated that the recovery stress resulted in a compressive force of approximately 700 lbs. However, when the heating was removed, the recovery stress was gradually lost.

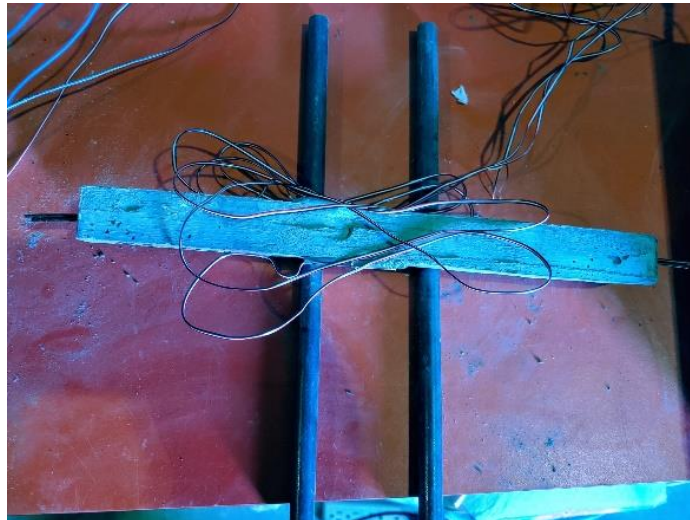**Figure 20. Test setup of Beam No. 3**
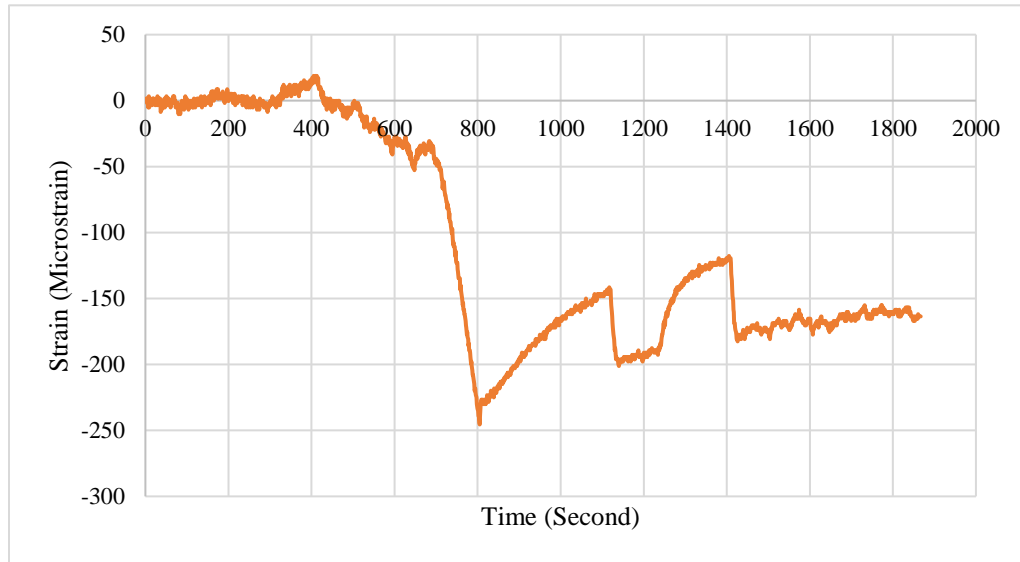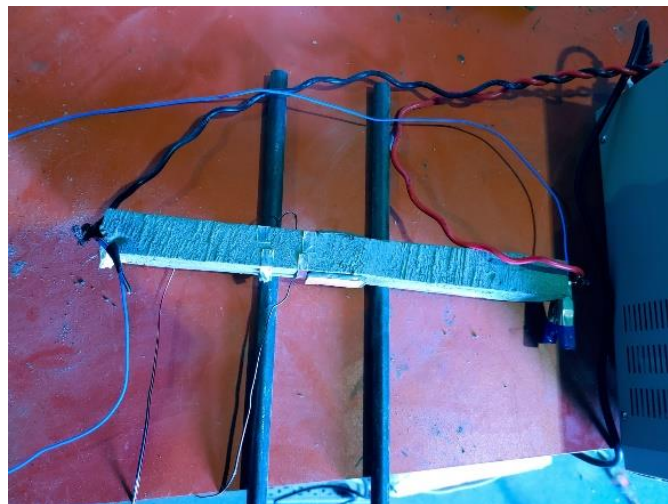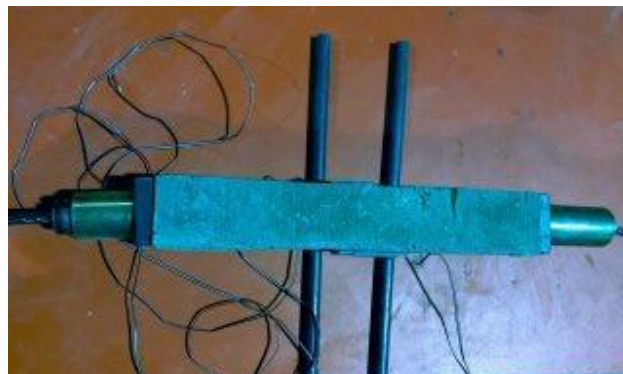
Figure 21. Test results of Beam No. 3
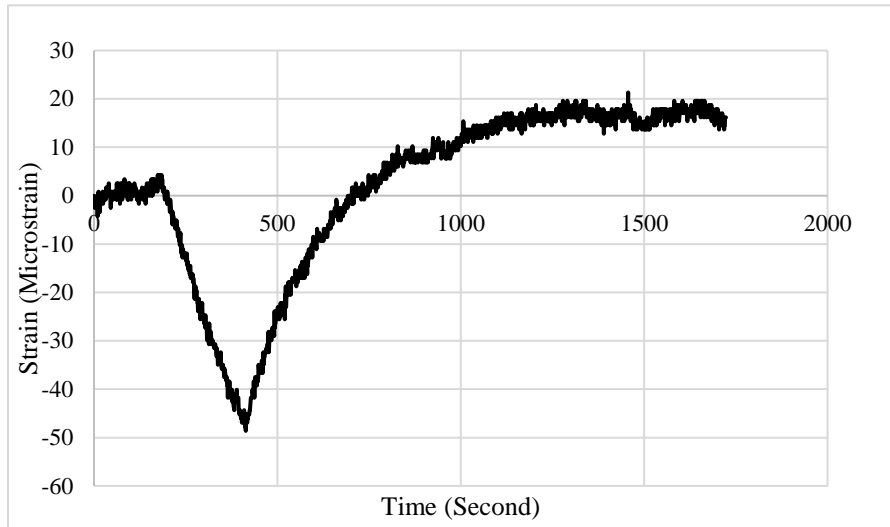
Figure 22 shows the test setup of Beam No. 4, in which one SMA cable was bonded with the concrete. One strain gauge was installed at each side face of the beam. Figure 23 plots the average readings from the two gauges versus time. When the cable was activated, the beam was subject to a maximum compressive strain of 10 microstrain, which corresponded to about 35 psi compressive stress in the concrete beam. It indicated that the recovery stress caused a compressive force of approximately 140 lbs. The recovery stress was relatively small primarily because of the short beam length, which was insufficient to develop the cable. Similarly to Figure 21, the recovery stress was gradually lost when the heating was removed.

Figure 22. Test results of Beam No. 4

Figure 23. Test results of Beam No. 4
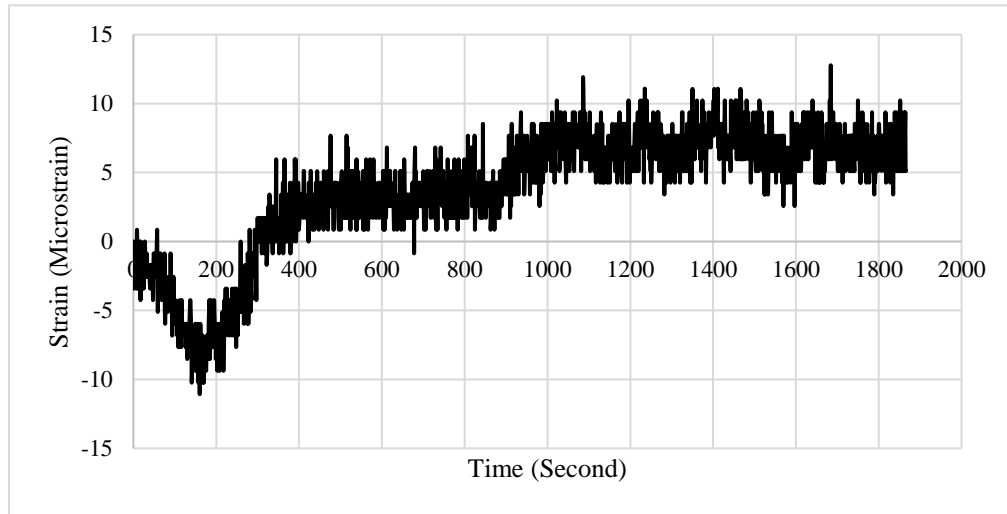
Full-scale Beam Test

A concrete beam was made in the lab to study the feasibility of using SMAs in eliminating end zone cracks at prestress release. As shown in Figure 24, the beam section is comparable to that of the AASHTO Type I beam and its flanges are simplified for ease of forming. The beam is 2 ft deep and its web is 6 in. wide. The beam flanges are 12 in. wide and 8 in. thick. The reinforcement included #4 stirrups in both flanges, pairs of #4 C-bars in the web, and #4 longitudinal bars. The C-bars were spaced at approximately 2 ft along the beam length except at the ends, in which two pairs were placed at 10 in. and 16 in. from each beam end, respectively. The shear reinforcement was intentionally provided far from the beam end to eliminate its contribution to the splitting resistance. The stirrups in the flanges were spaced at 4 in. for a distance of 2 ft from each beam end to provide sufficient confinement for the prestressing strands. Four 0.6 in.-diameter, Grade 270 strands were placed in flexible polymer plastic tubing in each flange. Figure 25 and Figure 26 show the beam's formwork and layout of the prestressing strands and reinforcing bars, respectively. Figure 27 shows the beam's end detail, in which three pairs of ½ in.-diameter PVC pipes were installed vertically in the beam web to house the SMA cables. Also shown are six SMA wires in the beam web.

Figure 24. Beam section and reinforcement detail
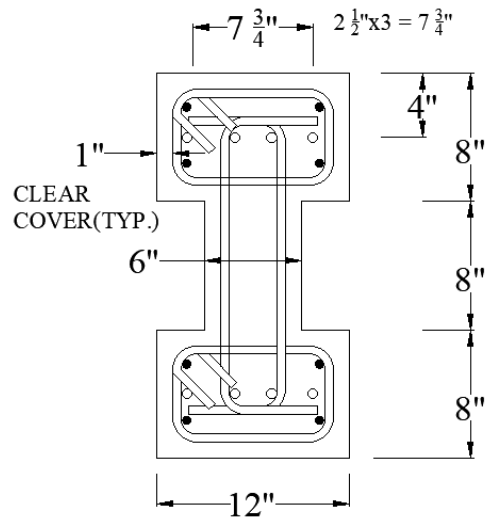
Figure 25. Beam formwork
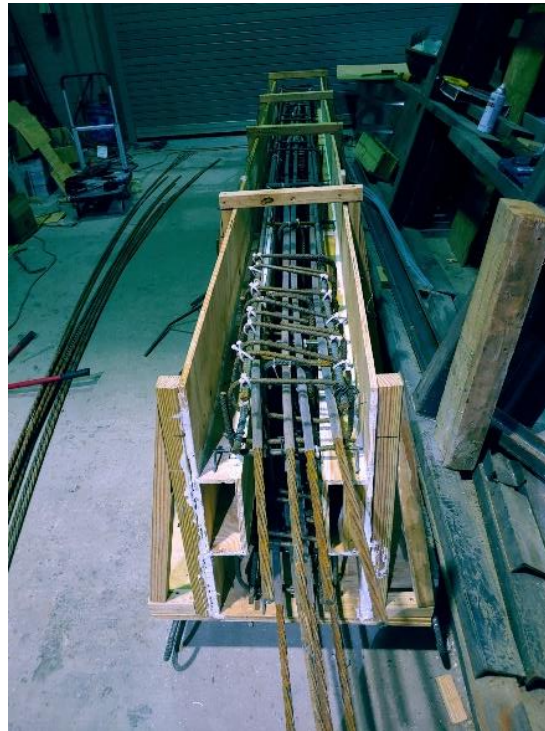
Figure 26. Reinforcement layout

Figure 27. Beam end detail

Ready-mix concrete was placed in the beam with a specified 28-day strength of 4,500 psi (Figure 28). The beam formwork was removed three days after the concrete pour (Figure 29) when the concrete strength reached about 3,300 psi based on the cylinder tests. Four SMA cables were eventually installed at one beam end and the cable ends were anchored by chucks. The first cable was electrically heated prior to installation of the other three cables. The heating was stopped after the cable's temperature reached approximately 100 ºC (Figure 30). The readings in the power supply are shown in Figure 31; the current was about 39 amps. Afterward, the other three cables were placed (Figure 32). Their distances measured to the beam end varied from 3 ½ to 9 in. to allow evaluation of their effect on

the splitting resistance (Figure 33). Because anchor set loss is significant for relatively shallow beams, all SMA cables were tensioned to about 770 lbs at the top to minimize its effect.

Figure 28. Concrete placement in the beam

Figure 29. Removal of beam formwork

Figure 30. Thermocouple reading of Cable 1

Figure 31. Readings in the power supply

Figure 32. Installation of all SMA cables

Figure 33. Layout of the SMA cables
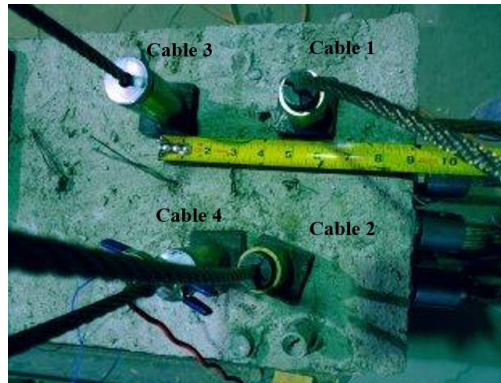
The longitudinal steel strands were post-tensioned four days after the concrete pour. The strands were numbered and tensioned in an order to remain symmetrical (Figure 34). Two strain gauges were installed at the end face of the beam web. Two other strain gauges were provided at the web side face, approximately 3 ft – 6 in. away from the beam end. However, they were accidentally damaged during beam handling. Figure 35 shows the placement of the mono-strand jack when a steel strand was tensioned. All strands were tensioned at one beam end following the sequence from Strand No. 1 to No. 8 as marked in Figure 34. As an average, each strand was jacked to approximately 32.2 kips. The strands were not fully tensioned to the allowable stress due to the relatively low concrete strength.

Figure 34. Numbering of the steel strands

Figure 35. Placement of the mono-strand jack

The readings of the two strain gauges at the beam end were collected and plotted in Figure 36 to Figure 38. Figure 36 shows the gauge readings when Cable 1 was electrically heated. The recovery stress resulted in approximately 15 microstrain at one gauge and 10 microstrain at the other gauge. As an average, these strains corresponded to approximately 44 psi compressive stress in the web. Similarly, Figure 37 illustrates the gauge readings when Cables 2 to 4 were electrically heated. Activating Cable 2 resulted in approximately 15 microstrain at both gauges. Because Cables 3 and 4 were located further from the beam end as compared to Cables 1 and 2, their effect was not so significant and caused approximately 10 microstrain. As a total, the four cables introduced about 40 microstrain or 139 psi compressive stress in the web. On the other hand, the recovery stress of the SMA wires was insignificant and therefore was not reported.

After all steel strands were tensioned, the gauge readings were approximately 80 microstrain (Figure 38), which corresponded to 279 psi tensile stress in the web. Because the modulus of rupture for concrete was about 431 psi, the resulting tensile stress was not high enough to crack the concrete. Therefore, no cracking was observed in the web.

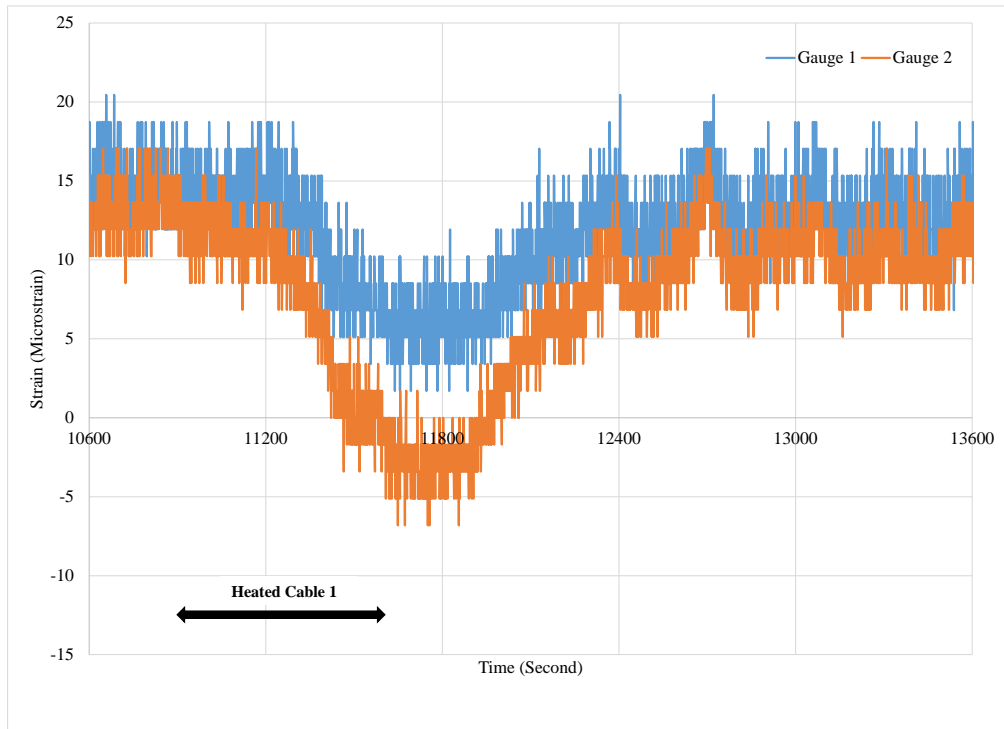**Figure 36. Gauge readings due to heating Cable 1**

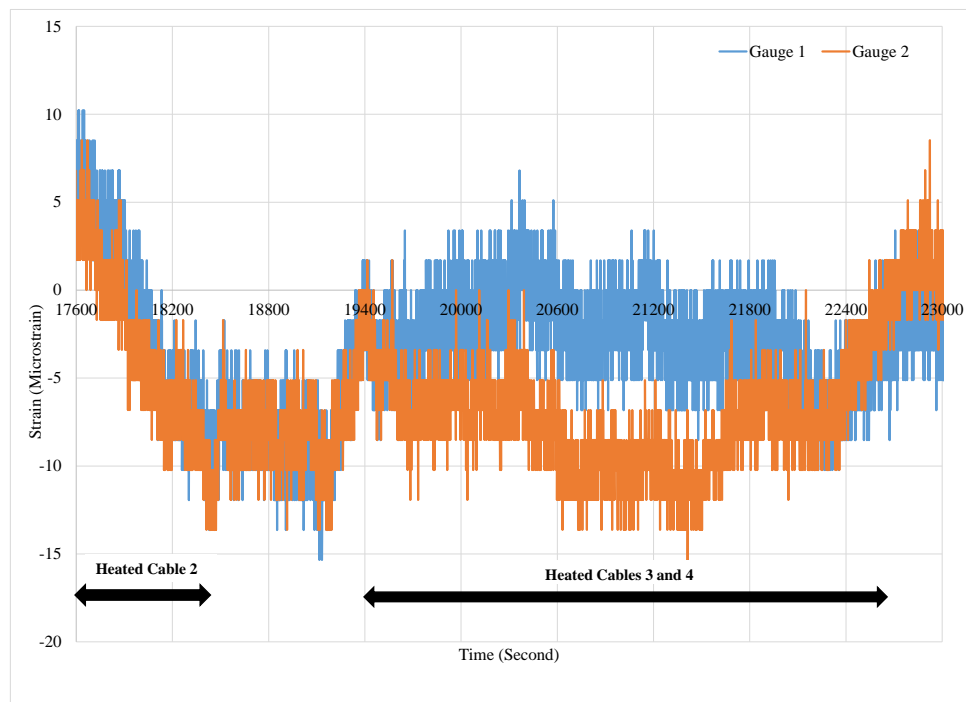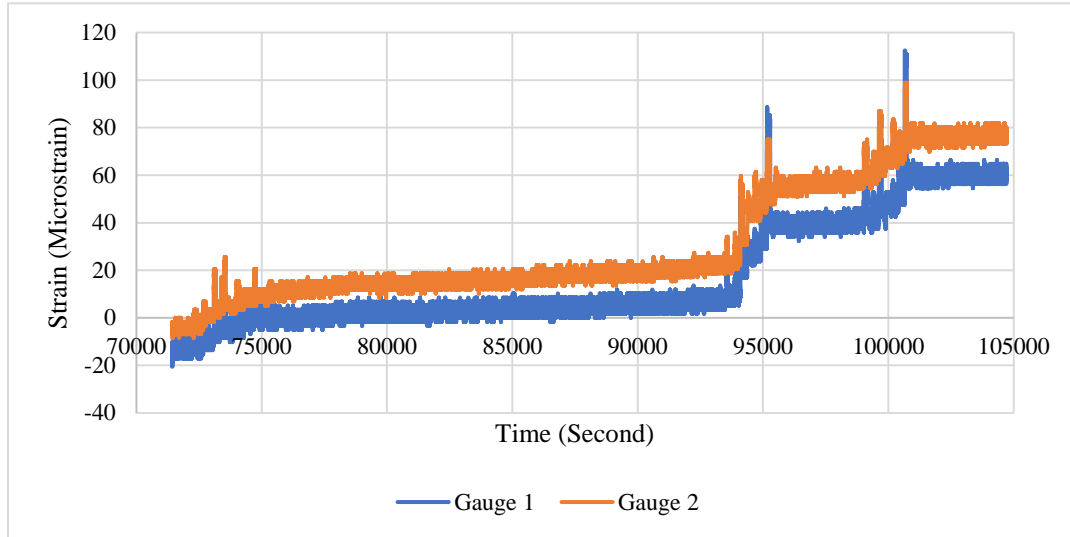**Figure 37. Gauge readings due to heating Cables 2 to 4**

Figure 38. Gauge readings due to tensioning steel strands

Finite Element Analysis

Finite element analysis (FEA) was conducted to simulate the behavior of the beam ends using ANSYS R19.2. The FEA model was developed to capture the end zone response when the SMA cables were activated and prestressing strands were released. Figure 39 shows the FEA model, in which half of the beam length was accounted for. The strain contour after activating Cable 1 is provided in Figure 40. It shows a strain of approximately 10 microstrain at one strain gauge, which is comparable to the collected gauge reading. Similarly, Figure 41 plots the strain contour after all cables are activated. The FEA model also accounted for the longitudinal prestressing force due to the steel strands. The analysis results were slightly higher than the strain gauge readings. The strain contour due to the combined effect between the longitudinal and vertical prestressing forces is shown in Figure 42. It confirms that the corresponding stresses in the web are less than the modulus of rupture for concrete.

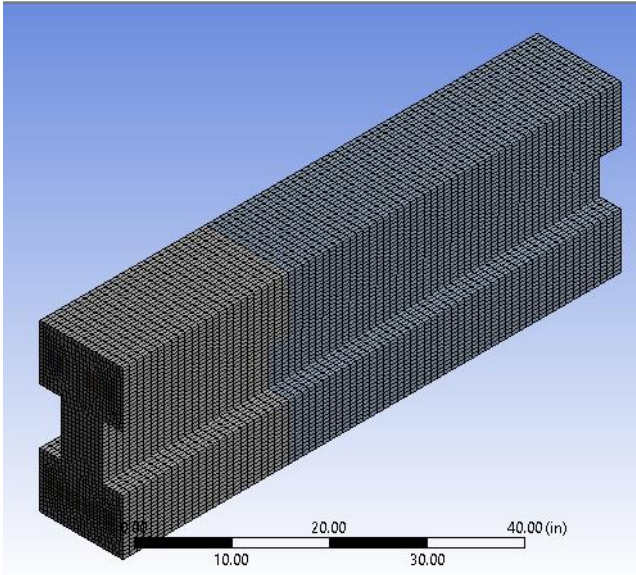**Figure 39. FEA model of the full-scale beam**
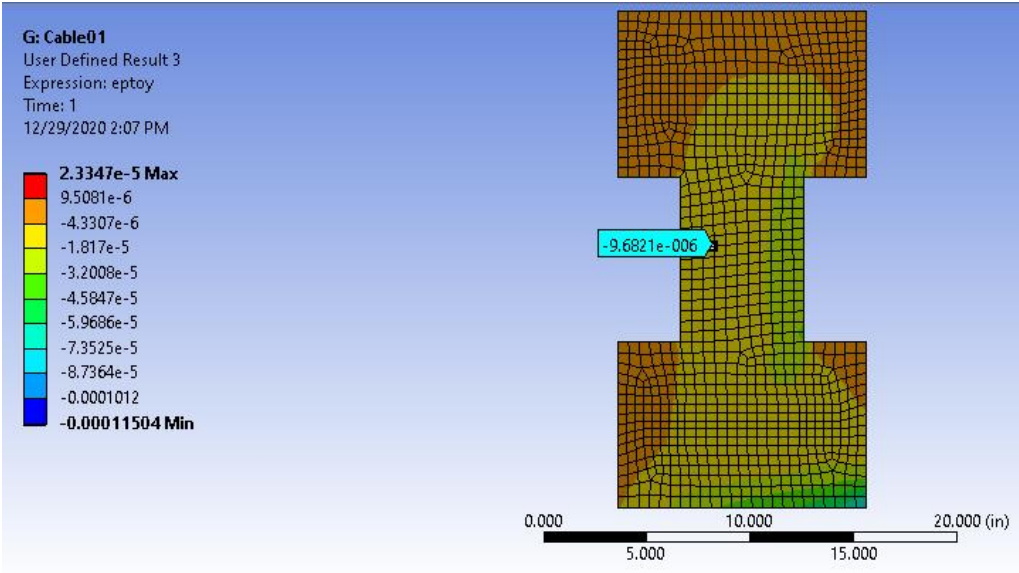

Figure 40. Strain contour after activating Cable 1

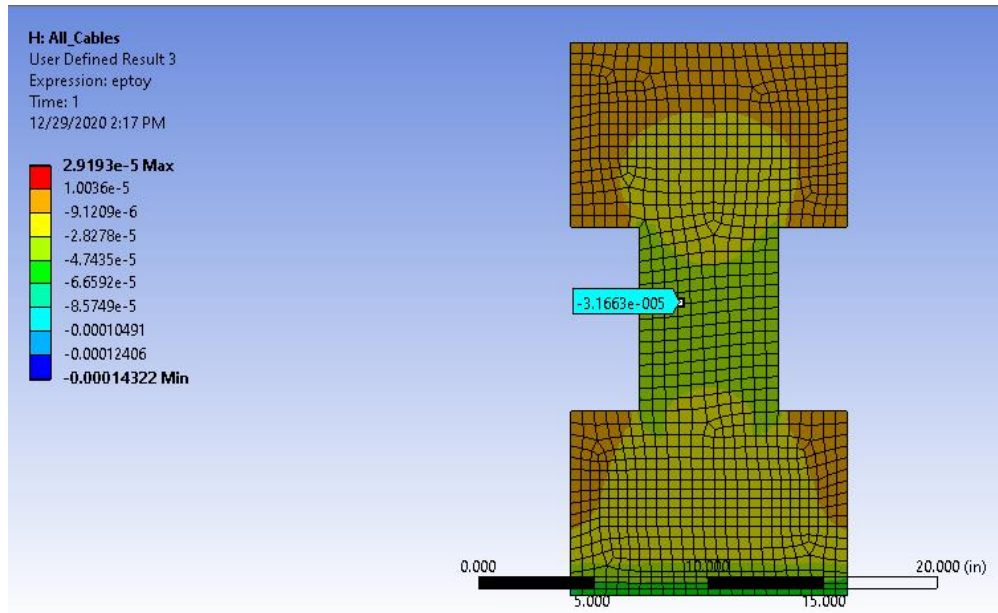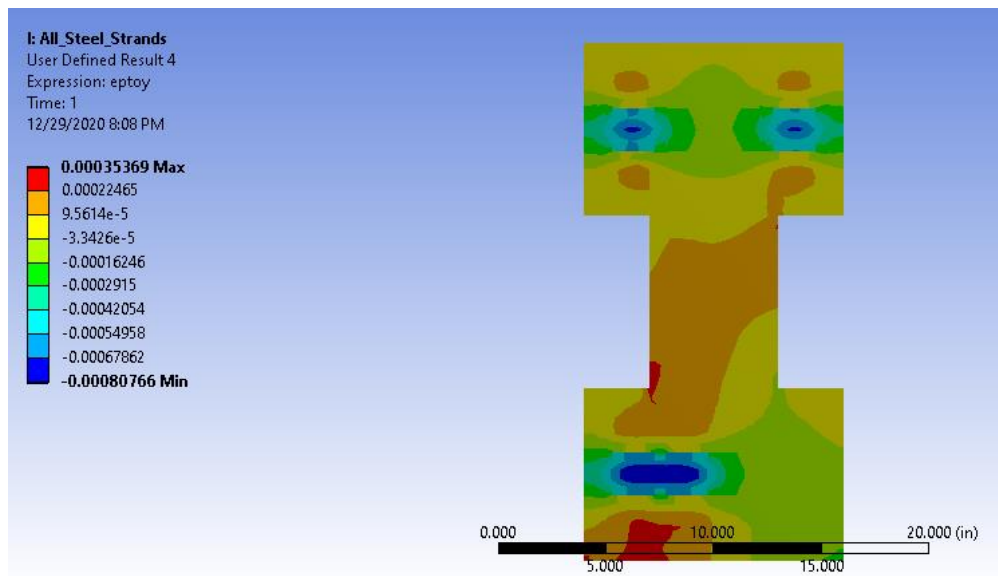**Figure 41. Strain contour after activating all cables**

Figure 42. Strain contour accounting for the effects of SMA cables and steel strands

Discussion of Results

This project explored the feasibility of using SMAs to introduce vertical prestress at a concrete beam end. Small-scale mortar and concrete beams were made using SMA wires, strands, and cables to evaluate their shape memory effect. A full-scale concrete beam was also produced to further verify the proposed concept. Finite-element analysis was performed to simulate the behavior of the beam end subject to both longitudinal and vertical prestressing forces, which resulted from the steel strands and SMA cables. The test and analysis results are discussed as follows:

1. Both heat gun and direct power supply were used to heat the SMAs at an early stage of the project. The heat gun was not effective because it did not provide uniform heating similar to the electrical heating option. A relatively high current up to 40 amps was necessary to heat the SMAs efficiently.

2. All beam tests showed that prestressing could be successfully introduced when the SMAs were activated.

3. The surface condition of the bonded SMAs apparently influenced the resulting prestress in the beam. The ends of the SMAs may be bent or anchored to leverage the recovery stress and maximize the prestressing.

4. The effectiveness of anchors for unbonded SMAs should be carefully selected to achieve desirable prestressing in the beam. Anchor set losses should be minimized when an unbonded system is implemented.

5. Some of the test results showed that the NiTi SMAs lost most of the recovery stress after the heat was removed. It indicates the need of selecting other SMAs, such as NiTiNb, that have a wide thermal hysteresis in real practices.

6. The provided SMA cables in the full-scale beam caused approximately 139 psi compressive stress in the web, indicating that the resulting prestressing force was significant. When properly designed, the SMAs can eliminate concrete cracking due to bursting forces at prestress release.

7. Finite element models can reasonably simulate the structural response of the beam end zone and account for the prestressing along both longitudinal and vertical directions.

Conclusions

Based on the lab testing and analysis results, the following conclusions are drawn:

1. The provided SMA cables in the full-scale beam resulted in appreciable compressive stress in the web.
2. The recovery stress of the NiTi cables was mostly lost after the electrical heating was removed. However, the lab testing validated the proposed concept of introducing vertical prestress through SMAs at the concrete beam ends.
3. Other types of SMAs, such as NiTiNb, seem to be more suitable in providing permanent prestressing with their wide thermal hysteresis.
4. When a SMA cable is located within a distance of $h/4$ (h = beam height) from the beam end, its contribution to the splitting resistance appears to be more effective.
5. The use of SMAs can successfully introduce vertical prestress at the prestressed concrete beam ends, and therefore can increase the splitting resistance and avoid concrete cracking at prestress release.

Recommendations

Precast prestressed concrete girders may exhibit cracking in the web due to the bursting forces at prestress release. This is particularly true for deep girders that involve a large number of prestressing strands. Use of unbonded SMA cables can provide a feasible solution to solve this challenge if a proper type of SMA is adopted. When SMA cables are electrically heated to provide the vertical prestress in concrete beams, their anchors should be carefully selected to minimize the anchor set losses and leverage recovery stress. The cable should be properly tensioned with one anchor in place prior to its installation such that the anchor set loss is totally eliminated. When the other anchor is installed on the beam, it should be seated as much as possible to reduce the seating loss. Further, it is necessary to locate the SMA cables within a distance of $h/4$ (h = beam height) from the beam end to maximize their contribution to the splitting resistance.

Acronyms, Abbreviations, and Symbols

Term	Description
AASHTO	American Association of State Highway and Transportation Officials
LRFD	load-and-resistance factor design
ft.	foot (feet)
in.	inch(es)
in.^{2}	square inch(es)
LADOTD	Louisiana Department of Transportation and Development
LTRC	Louisiana Transportation Research Center
lb.	pound(s)
m	meter(s)
MPa	Megapascal
ksi	kilo-pound per square inch
psi	pound per square inch
NCHRP	National Cooperative Highway Research Program
NiTi	nickel-titanium
NiTiNb	Nickel-titanium-niobium

References

[1] P. Okumus and M. Oliva, "Evaluation of crack control methods for end zone cracking in prestressed concrete bridge girders," *PCI Journal,* vol. 58(2), 2013.

[2] M. Tadros, S. Badie and C. Tuan, "Evaluation and repair procedures for precast/prestressed concrete girders with longitudinal cracking in the web (Vol. 654)," Transportation Research Board, 2010.

[3] AASHTO, AASHTO LRFD Bridge Design Specifications, Ninth Edition, Washington, D.C., 2020.

[4] O. Ozbulut and R. Hamilton, "Smart Concrete Bridge Girders Using Shape Memory Alloys," Mid-Atlantic Universities Transportation Center, 2015.

[5] M. Alam, M. Youssef and M. Nehdi, "Utilizing shape memory alloys to enhance the performance and safety of civil infrastructure: a review," *Canadian Journal of Civil Engineering,* vol. 34(9), pp. 1075-1086, 2007.

[6] A. Maji and I. Negret, "Smart prestressing with shape-memory alloy," *Journal of engineering mechanics,* vol. 124(10), pp. 1121-1128, 1998.

[7] S. El-Tawil and J. Ortega-Rosales, "Prestressing concrete using shape memory alloy tendons," *Structural Journal,* vol. 101(6), pp. 846-851, 2004.

[8] M. Sherif, O. Ozbulut, A. Landa and R. Hamilton, "Self-post-tensioning for concrete beams using shape memory alloys," in *Proceedings of the ASME Smart Materials, Adaptive Structures and Intelligent Systems (Vol. 46155, p. V002T04A014)*, 2014.

[9] K. Moser, A. Bergamini, R. Christen and C. Czaderski, "Feasibility of concrete prestressed by shape memory alloy short fibers," *Materials and Structures,* vol. 38(5), pp. 593-600, 2005.

[10] P. Soroushian, K. Ostowari, A. Nossoni and H. Chowdhury, "Repair and strengthening of concrete structures through application of corrective

posttensioning forces with shape memory alloys," *Transportation Research Record,* vol. 1770(1), pp. 20-26, 2001.

[11] B. Andrawes, "Adaptive prestressing system for concrete crossties (No. Rail Safety IDEA Project 33)," 2019.

[12] A. Sinha, N. Tatar and J. Tatar, "Rapid heat-activated post-tensioning of damaged reinforced concrete girders with unbonded near-surface mounted (NSM) NiTiNb shape-memory alloy wires," *Materials and Structures,* vol. 53(4), pp. 1-15, 2020.